

Taphonomic-forensic analysis of the hominin skulls from the Sima de los Huesos

Nohemi Sala^{1,2}  | Ana Pantoja-Pérez^{1,2} | Ana Gracia^{2,3} | Juan Luis Arsuaga^{2,4}

¹Centro Nacional de Investigación sobre Evolución Humana-CENIEH, Burgos, Spain

²Centro Mixto UCM-ISCIII de Evolución y Comportamiento Humanos, Madrid, Spain

³Departamento de Geología, Geografía y Medio Ambiente, Universidad de Alcalá, Alcalá de Henares, Spain

⁴Departamento de Geodinámica, Estratigrafía y Paleontología, Facultad Ciencias Geológicas, Universidad Complutense de Madrid, Madrid, Spain

Correspondence

Nohemi Sala, Centro Nacional de Investigación sobre Evolución Humana-CENIEH, Paseo de la Sierra de Atapuerca, 3, 09002 Burgos, Spain.
Email: nohemisala@cenieh.es

Funding information

CaixaBank-Fundación Atapuerca; H2020 European Research Council (ERC-STG-DEATHREVOL), Grant/Award Number: 949330; Ministerio de Ciencia, Innovación y Universidades (MCI/AEI/FEDER, UE), Grant/Award Numbers: PGC2018-093925-B-C33, RYC2020-029656-I

Abstract

The Sima de los Huesos (SH) hominin assemblage is composed of thousands of fossil fragments, including pieces of crania and mandibles. The main objective of this work is to address the main taphonomic features of the cranial and mandibular remains from the SH sample, including antemortem, perimortem, and postmortem skeletal disturbances. We present an updated assessment of healed cranial trauma, first described in 1997 and now including new skulls. In addition, this study reviews the perimortem fractures in relation to their location and features of the affected individuals. Finally, this paper deals with the modifications affecting the cranial sample from the SH at the postmortem stage, including physical and biological postdepositional modifications. The SH collection provides a unique opportunity for conducting a complete forensic-taphonomic study on a Middle Pleistocene population.

KEY WORDS

bone trauma, cranial trauma and breakage, middle Pleistocene hominins, taphonomy

1 | INTRODUCTION

The Paleolithic fossil record, does not commonly provide an opportunity to perform a population-level taphonomic analysis. If we go back to the Middle Pleistocene, this kind of analysis is practically impossible, because hominin fossils from earlier than the Late Pleistocene are generally scarce. Furthermore, they are geographically and chronologically dispersed and bone assemblages representing the same biological population are infrequently found. Excluding the cannibalism assemblages (de Lumley, 2015; Saladié et al., 2012), in the best of cases isolated fossils can be characterized taphonomically (Sanz et al., 2018), with one exception: La Sima de los Huesos (SH). The SH hominin assemblage is composed of more than 7,000 fossil fragments

derived from 29 individuals (Bermúdez de Castro et al., 2021). The SH site provides a significant opportunity to carry out a complete forensic-taphonomic study on a Middle Pleistocene population. It is necessary to apply both taphonomic and forensic criteria in order to identify antemortem, perimortem, and postmortem disturbances to the SH skull sample.

The SH site has been the object of forensic-taphonomic studies since the first findings of human fossils there (Andrews & Fernández-Jalvo, 1997; Arsuaga et al., 1990, 1997). Antemortem cranial injuries have been described previously by Pérez (1989, 1991); Pérez et al. (1997). Sala, Arsuaga, et al. (2014) performed bone surface modification analyses of cranial and postcranial remains, focusing on carnivore bone modifications in

particular. The first detailed studies on fractures in SH were published by Sala et al. (Sala, Arsuaga, Martínez, et al., 2015; Sala, Arsuaga, Pantoja-Pérez, et al., 2015; Sala, Pantoja, et al., 2014) in which an in-depth methodological proposal was summarized, thus addressing the study of fractures in cranial remains from the fossil record.

The main objective of this study is to create a catalog of modifications to crania and mandibles within the SH sample, including antemortem, perimortem, and postmortem skeletal disturbances, at a populational level. This includes incorporating the new recovered remains, thereby updating some aspects that were already covered in previous research. In other cases, the present study delves into taphonomic aspects, especially in relation to antemortem and postmortem processes.

2 | MATERIALS AND METHODOLOGICAL PROCEDURE

For the taphonomic analysis of the SH skull sample, all skull fragments (number of identified specimens = 2,035) have been considered. Of these, 1,900 correspond to cranial fragments, of which around 670 fragments have been fitted together to form a minimum number of elements (MNE) of 20 crania (named Cr-1 to Cr-20), and 132 mandibular fragments comprise a MNE of 20 so far. Cr-1 to Cr-17 have been described previously (Arsuaga et al., 2014) and references therein), but three new cranial individuals (Cr-18 to Cr-20) have been described for the first time in this volume (Pantoja-Pérez & Arsuaga, n.d.).

The bone surfaces were scrutinized at both macro- and microscopic levels under a binocular device (Nikon SMZ800) and a DINO-LITE digital microscope. In addition to the direct study of the fossils, we performed taphonomic and forensic analyses based on virtual reconstructions. CT scanning and 3D virtual imaging provide an opportunity to study critical aspects of fracture features, especially when the different bone fragments are glued together (Gómez-Olivencia et al., 2018; Pantoja-Pérez et al., 2016; Sala et al., 2016; Sanz et al., 2018). In this work, we examine the timing of each fracture as antemortem (i.e., before death), perimortem (i.e., at or around the time of death), and postmortem fractures (i.e., occurring long after death) in cranial remains. To determine the timing of cranial bone fracturing and the possible causes of perimortem injuries (accidental vs. intentional) of skull bone fractures within the SH sample, we focused on the calvaria. The parietal, occipital and frontal bones are characterized by outer and inner tables of dense cortical bone separated by a trabecular diploë, which are more diagnostic than the thinner

cranial bones of the splanchnocranum. In addition, the mandibular fragments have been considered in assessing the timing of the fracture. We studied the following parameters: presence of healing, fracture type (linear, depressed, stellate, or mixed depressed/stellate), fracture location, fracture trajectory (noncrossing or crossing suture lines), fracture angle (right or oblique), presence/absence of cortical delamination, and edge texture (smooth or jagged), according to Sala et al. (2016) and references therein.

For the characterization of antemortem trauma, we measured maximum length and breadth of the injuries, as well as perimeter and area, using DINO-LITE software tools (DinoXcope 2.0). For the visualization and measurements of the internal structure of cranial injuries, CT images of the crania were used. The crania were CT scanned in the coronal plane using an industrial YXLON MU 2000-CT scanner at the Universidad de Burgos (Spain). Virtual (3D CT) models of each cranium were generated from the resulting slices using the Mimics 18.0 (Materialize N.V.) software package. For the analysis of the distribution of cranial injuries, we located the centroid of each injury, based on X, Y, and Z coordinates in a standardized skull template of SH. The skull template was created by virtually reconstructing Cr-17 by mirroring the missing areas of the skull. The X, Y, and Z coordinates of the injuries were given as landmarks in the Mimics software. The location and distribution of cranial injuries (antemortem and perimortem trauma) were analyzed using the QGIS (v. 3.18.3) software package. We used the heatmap tool to study the distribution of the cranial injuries. The heatmap plugin uses Kernel Density Estimation to create a density heatmap. The density is calculated based on the number of points in a location, with larger numbers of clustered points resulting in larger values. Heatmaps allow easy identification of “hot-spots” and clustering of points (QGIS.org, 2021).

In cases where there are dental individuals associated with cranial specimens, the age at death and the sex estimation according to the dental pieces have been considered in accordance with Bermúdez de Castro et al. (2021). In the case of individuals lacking associated dentition, their sex estimation and age at death have been calculated following Arsuaga et al. (2014) and Pantoja-Pérez and Arsuaga (n.d.). The completeness index has been calculated as a preserved percentage considering the bones forming the cranial vault where traumas are located: frontal, both parietals, and the occipital squama of the occipital bone (above the lower nuchal crest). For the analysis of antemortem trauma in relation to the collection's demographic data and the completeness index, the Mann-Whitney test (Mann & Whitney, 1947) and the correlation test were performed, respectively.

3 | BONE FRACTURE AND TRAUMA ANALYSES

3.1 | Antemortem injuries

Antemortem injuries are distinguished based on signs of healing or bone remodeling. This includes abnormal bone growth, callus formation, abnormal bone shape, or characteristics associated with an infection (Kimmerle & Baraybar, 2008).

Pérez et al. (1997) described 14 cranial injuries as “cranial erosions with an oval or subcircular shape.” They contemplated that these lesions responded to inflammatory processes affecting the scalp and consequently the external table of the cranial bones (Pérez et al., 1997). However, they stated that it was not possible to determine whether they were caused by blows or generalized scalp infections. Nevertheless, in the case of

frontal bone AT-764 (currently belonging to Cr-11) the lesion detected in the left orbit (Figure 1) was clearly considered a traumatic lesion with signs of healing (Pérez et al., 1997). Also, Cranium 5 has evidence of bone pathology in the maxilla caused by trauma that produced a chronic infection (Gracia et al., 2013).

The cranial remains sample is now larger, and 57 subcircular lesions have been recognized (Table 1). The cranial injuries located at the calvaria are oval or circular in shape (Figure 1) and ranged from 3 mm to 2 cm diameter (Table 1). The lesions appear as depressed areas whose texture is characterized by porosity formed by vascular holes penetrating through the cortical bone, as a remodeled woven bone. Lesion borders are usually well-delimited, and sometimes a step morphology or concentric ring is observed (Figure 1). The CT sectional images show that the lesions affect the external table of the cranial bones (Figure 2) and in some cases also affect the



FIGURE 1 Some examples of healed antemortem trauma of several cranial individuals

TABLE 1 Inventory and description of the healed injuries in the SH cranial sample

Specimen	No. injury	Location	Area (mm²)	Perimeter	Max. diameter	Min. diameter
Cranium 1	C1-1	Right part of the occipital squama	-	-	-	-
Cranium 2	C2-1	Anterior part of the left parietal	62.8	27.6	9.7	8.5
	C2-2	Anterior part of the right parietal	21.2	16.4	5.9	4.7
Cranium 3	C3-1	Posterior part of the right parietal, close to the sagittal suture	83.5	32.9	11.4	9.6
Cranium 4	C4-1	Occipital squama, right to the suprainiac area	170.6	47.9	17.0	13.0
Cranium 5	C5-1	Left supraorbital torus	85.7	35.0	13.2	8.6
	C5-2	Left supraorbital torus	50.6	28.6	11.0	6.3
	C5-3	Left part of the frontal squama	15.6	14.5	5.4	4.1
	C5-4	Right part of the frontal squama	34.9	21.5	7.3	6.2
	C5-5	Right parietal, close to bregma	61.9	30.4	11.8	6.4
	C5-6	Right parietal, close to lambdatic suture	61.8	31.7	13.1	5.6
	C5-7	Anterior part of the right parietal, above the temporal lines	-	-	-	-
	C5-8	Posterior part of the right parietal, between the sagittal suture and the parietal protuberance	35.8	24.5	10.9	4.4
	C5-9	Posterior part of the left parietal, above lambdatic suture	35.3	21.5	7.5	6.4
	C5-10	Posterior part of the left parietal, above lambdatic suture and close to the temporal lines	121.0	40.8	14.4	11.3
	C5-11	Near the left parietal eminence	-	-	-	-
	C5-12	Near the left parietal eminence	-	-	-	-
	C5-13	Left parietal, close to the temporal lines	-	-	-	-
	C5-14	Right part of the occipital squama, near the lambdatic suture	98.6	36.6	13.7	9.5
	C5-15	Occipital squama above the suprainiac area	57.0	27.7	10.0	7.4
Cranium 6	C6-1	Right part of the frontal squama, behind the supraorbital torus	36.1	22.6	8.5	5.3
	C6-2	Left parietal, close to the coronal suture	20.0	16.8	6.4	3.9
Cranium 7	C7-1	Posterior part of the left parietal, close to the sagittal suture	65.2	29.4	11.1	7.9
	C7-2	Coinciding with lambda	46.7	25.1	9.2	6.3
Cranium 8	C8-1	Posterior part of the left parietal, close to lambdatic region	65.5	29.6	10.2	7.2
	C8-2	Posterior part of the left parietal, close to lambdatic region	60.0	28.1	9.5	8.4
Cranium 9	C9-1	Right part of the frontal squama	79.0	33.1	13.0	7.7
	C9-2	Left parietal, close to bregma	24.9	18.0	6.0	5.9
	C9-3	Right part of the frontal squama	13.1	13.4	5.1	3.3
Cranium 10	C10-1	Middle plane of the frontal squama	28.0	19.2	6.8	5.2
	C10-2	Middle plane of the frontal squama	89.6	34.7	12.6	9.0
Cranium 11	C11-1	Above the left supraorbital torus	201.8	55.9	23.0	11.0
	C11-2	Right parietal, close to the coronal suture	27.9	19.6	7.4	4.9

TABLE 1 (Continued)

Specimen	No. injury	Location	Area (mm ²)	Perimeter	Max. diameter	Min. diameter
Cranium 12	C12-1	Right parietal, close to temporal lines	-	-	-	-
Cranium 13	C13-1	Frontal squama, close to coronal suture	140.3	46.2	19.0	9.5
	C13-2	Right parietal, between lambda and parietal eminence	44.8	24.2	8.5	6.7
	C13-3	Asterion region of the left parietal	16.0	14.8	5.2	3.8
Cranium 14	C14-1	Right part of the frontal squama	182.3	48.8	15.9	13.8
	C14-2	Left part of the frontal squama	36.8	23.9	9.7	4.9
	C14-3	Near the right parietal eminence	42.1	23.9	8.6	6.3
	C14-4	Above the frontal trigon	-	-	-	-
	C14-5	Left parietal eminence	-	-	-	-
Cranium 15	C15-1	Middle of the left parietal, near the sagittal suture	144.6	43.4	14.4	12.5
	C15-2	Posterior part of the left parietal, near the sagittal suture	49.7	25.3	8.5	7.6
	C15-3	Middle of the left parietal, near the sagittal suture	17.6	15.4	5.6	4.4
	C15-4	Posterior part of the left parietal, near the sagittal suture	50.7	26.0	8.9	7.5
	C15-5	Posteromedial quadrant of the left parietal	83.2	37.8	16.1	7.0
	C15-6	Middle of the left arch of the lambdatic suture	221.9	57.3	21.1	13.1
	C15-7	Posterolateral quadrant of the left parietal, close to temporal lines	81.0	43.0	19.0	5.2
	C15-8	Posterolateral quadrant of the left parietal	43.9	31.0	13.1	4.6
	C15-9	Asterion region of the left parietal	29.1	22.1	9.4	4.1
	C15-10	Middle of the left parietal, on the temporal lines	242.7	55.7	18.8	15.1
	C15-11	Middle of the left parietal, on the temporal lines	138.3	46.2	14.8	11.9
Cranium 16	C16-1	Left part of the frontal squama	29.2	24.0	10.5	3.5
	C16-2	Occipital squama, right and upward of the suprainiac area	41.3	23.2	7.8	6.4
	C16-3	Right parietal, close to the parietal eminence	-	-	-	-
Cranium 17	C17-1 ^a	Right parietal, close to bregma	21.4	21.3	7.7	3.0
Cranium 19	C19-1	Left half of the frontal squama	18.7	16.7	5.5	4.0

Note: When the injuries are not well-defined, measurements are not given. In Cranium 1, there is an injury whose contour is eroded but was previously published in Pérez et al. (1997) as an injury with a 9-mm perimeter.

^aPartially preserved.

diploë. The injuries appear in virtually all analyzed cranial individuals (17/20 skulls). In some cases, individuals showed only one lesion (e.g., Cr-3, Cr-4, or Cr-12); in other cases, however, such as Cr-15 or Cr-5, more than 10 healed injuries were documented (Table 1).

Different circumstances can produce bone abnormalities of the cranial bones, including dietary deficiencies (anemia), infectious disease (such as syphilis or tuberculosis),

tumors (osteoblastomas, meningiomas, and hemangiomas), burning, and trauma (Shang & Trinkaus, 2008; Wu et al., 2011). Nontraumatic diseases seem an unlikely explanation for these lesions based on the following criteria: (a) the absence of diploic expansion in all of the cases analyzed allows us to rule out anemia-related porotic hyperostosis (Ortner, 2003). (b) Infectious diseases such as syphilis or tuberculosis usually manifest as lytic processes resulting

in multiple small areas of bone destruction in both cranial (splanchnocranum and neurocranium) and postcranial remains (Ortner, 2003; Shang & Trinkaus, 2008). There is no sign of bone destruction in the SH individuals' facial skeletons, mandibles, or the postcranial skeleton of any individual, rendering mycobacterial or treponemal diseases unlikely causes. (c) Although tumors can cause alterations in the cranial vault, it is more common for them to affect the diploë and endocranial table according to Shang and Trinkaus (2008) and references therein. On the other hand, it is very unlikely that tumors affected almost all of the cranially preserved individuals in the SH population. (d) The total absence of thermal alteration marks on the skulls prevents us from interpreting these lesions as the result of burning. Therefore, the hypothesis that best explains the existence of these lesions would be blunt force impacts that caused depressions on the outer table of the skulls leading to subsequent bone remodeling on the outer table and, on some occasions, on the diploë.

Thus, the SH healed injuries could be considered depressed fractures (Lovell, 1997; Ortner, 2008). Depression fractures in the cranium are characterized by their subcircular shape, mainly affecting the outer table and causing a depression at the point of impact. On healed injuries, a circular depression remains on the outer surface and the bone remodeling is evident (Figure 1). Following Ortner and Putschar (1981), depressed fractures that occur during life tend to have less defined edges than

those resulting from postmortem damage. Blunt force trauma from compression results in depressed fractures, and penetrating defects with or without radiating fractures. Depressed fractures usually occur when an object strikes the skeletal surface (Kimmerle & Baraybar, 2008). In fact, clinical examples show that depression fractures may be created in bone as the result of hammer blows and/or falls onto sharp edged objects (Lovell, 1997).

In sum, the cranial injuries described in Table 1, which affect practically all the SH cranial individuals, are compatible with healed depression fractures. This suggests that this population was subjected to numerous episodes that caused nonfatal blunt impacts throughout their lives. The antemortem lesions of 20 cranial individuals are concentrated in the calotte, in those bony regions that are not covered by the masticatory or nuchal musculature, more specifically, in the most exposed areas of the skull, only covered by the scalp (Figure 3). The lesions are mainly present above the hat brim line (HBL zone, see Kremer et al. (2008); Kremer and Sauvageau (2009); Sala et al. (2016)), affecting both the right and left side, though they seem to occur more frequently on the left side (Figure 3).

Considering the demographic data of the cranial collection (sexual and age estimation), as well as the completeness index (calculated as a percentage of the calvarum preservation), we observe that there are no significant statistical differences between the incidence of

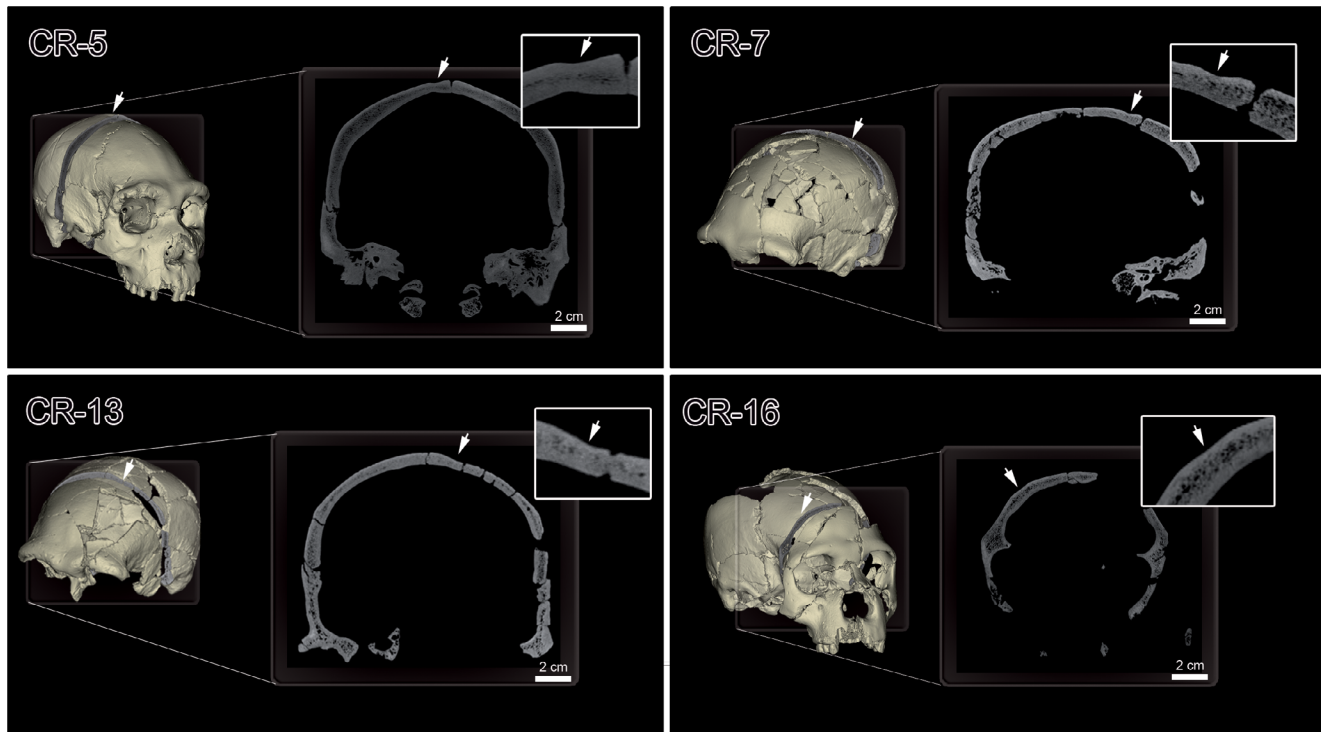


FIGURE 2 CT images of Cr-5, Cr-7, Cr-13, and Cr-16 showing the antemortem injuries that allow for observation of their effects on the external table and diploë

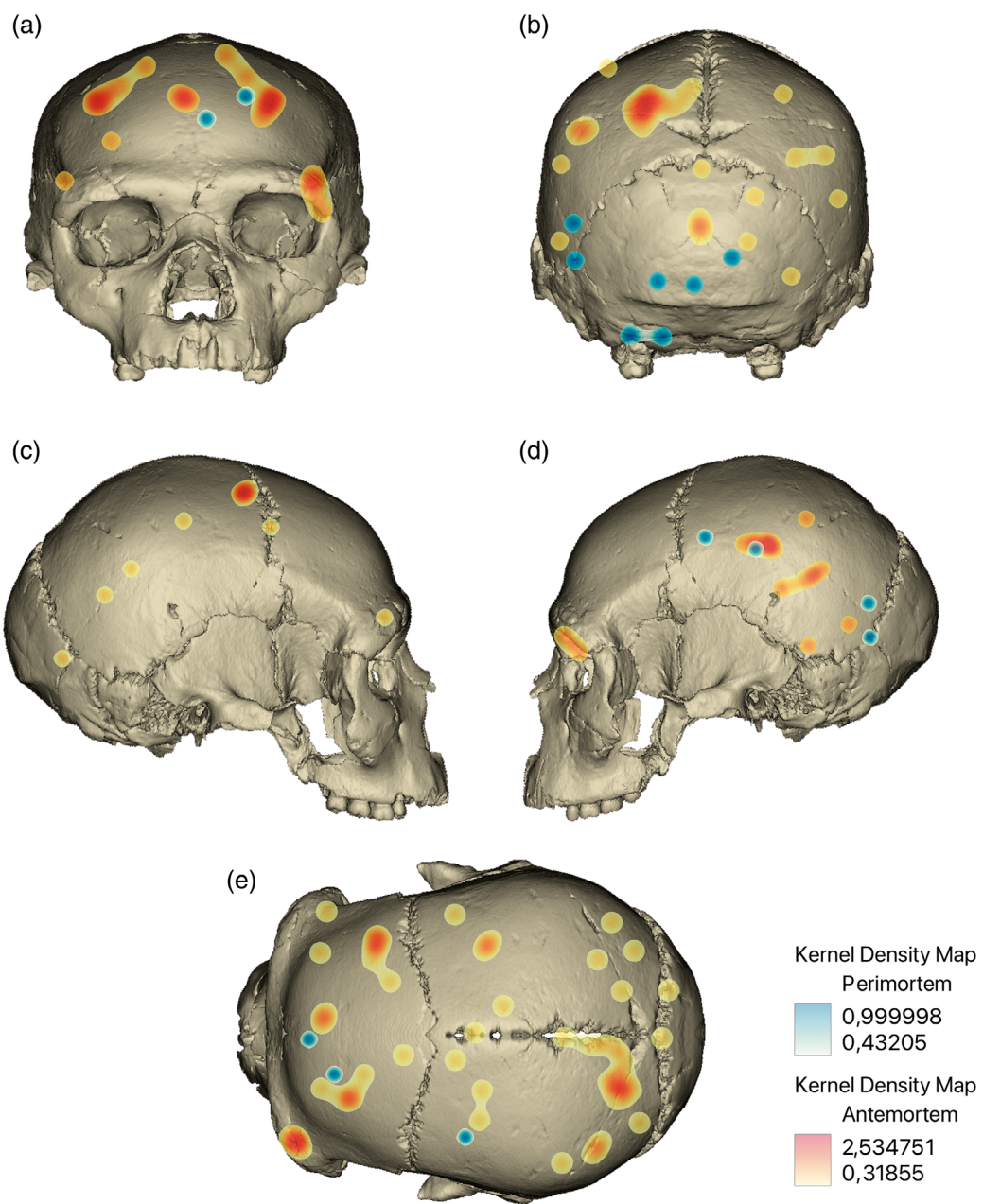


FIGURE 3 Heatmap results showing the location and density of antemortem (warm colors) and perimortem (cool colors) for the frontal (a), occipital (b), right (c), left (d), and superior (e) views of the Sima de los Huesos crania

antemortem injuries and age ($p > .05$), sex estimation ($p > .05$), or correlation with the completeness index ($r^2 = .14$; $p = 0.1$) (see Table S1). Therefore, there is no evident relationship between the incidence of head injuries and age or sexual assignment categories.

3.2 | Perimortem fractures

Perimortem fractures occur while the bone is still fresh (i.e., surrounded by soft tissue and/or preserving the organic matrix) (Ortner, 2008; Ubelaker & Adams, 1995)

and exhibit no evidence of healing. Perimortem injuries occur at the time of death, but they can also occur after death, while the body still preserves soft tissue. Perimortem fractures can help to identify the cause of death (accidental, such as free-falls or violence-related) or whether the processes happened shortly after death (Martin & Harrod, 2015).

In order to identify when the fracture occurred, an in-depth analysis of the cranial fractures was necessary. Perimortem fractures can be identified by oblique angles, smooth surfaces, the presence of cortical delamination, a pattern of depressed fracture outlines, and fractures

crossing cranial sutures (Sala et al., 2016 and references therein). Sala et al. (2016) documented perimortem fractures in eight crania from SH: Cr-3, Cr-5, Cr-7, Cr-9, Cr-11, Cr-13, Cr-14, and Cr-17. In addition, the new immature cranium described in this volume, CR-18 (Pantoja-Pérez & Arsuaga, n.d.), also shows a fracture with features compatible with perimortem trauma (e.g., a circular outline, oblique angles, and cortical delamination). Therefore, a total of nine individuals, out of the 20 that are currently in the collection, display evidence of perimortem trauma. Different patterns in perimortem fractures, in terms of type of injuries and location, can be distinguished in the SH cranial collection (Figure 3). First, depressed fractures in the left parietal bones above the HBL in Cranium 5 (Cr-5) and Cranium 11 (Cr-11) (Figure 3) can be observed. The type of fractures and their location are compatible with violence-related injuries (Sala et al., 2016). The second pattern is the most frequent among the perimortem injuries from SH (six of nine crania with perimortem injuries) and consist of penetrating fractures of circular morphology in the nuchal region of the crania (Figures 3–6).

Cr-3 and Cr-7 (Figure 4), Cr-9 and Cr-13 (Figure 5), Cr-14 (Figure 6) and Cr-18 display penetrating fractures with oblique angles (beveling on the inner table) and cortical delamination, as well as a smooth surface. Penetrating fractures may result from both low and high velocity projectiles (Thomas, 1984). In most cases, they are located in the occipital bone near the left asterion (Figure 3).

The last pattern is represented by a single individual. Cranial individual Cr-17 displays two perimortem traumas in the frontal bone (Figure 6). The dimensions and contours of the two depression fractures were found to be almost indistinguishable (including the presence of a similarly-placed notch in both fracture outlines), strongly suggesting that both fractures were caused by the same object. Finally, the fractures show different orientations and different trajectories, thus implying that each fracture was caused by an independent impact (Sala, Arsuaga, Pantoja-Pérez, et al., 2015). All these data demonstrate that the Cr-17 blunt force traumas clearly are not accidental, but rather they appear to have been produced by the use of a tool of standardized size and



FIGURE 4 Perimortem penetrating wounds in Cranium-3 and Cranium-7. Observe the detailed endocranial and ectocranial views of the injuries. Note beveling and cortical delamination around the defects along the inner table

FIGURE 5 Perimortem penetrating wounds in Cranium-9 and Cranium-13. Observe the detailed endocranial and ectocranial views of the injuries. Note beveling and cortical delamination around the defects along the inner table



shape and, thus, the most plausible explanation for the perimortem fractures on Cr-17 is that they are the result of intentional and repeated blows during a lethal act of interpersonal violence (Sala, Arsuaga, Pantoja-Pérez, et al., 2015).

3.3 | Postmortem fractures

The postmortem cranial fractures occur on defleshed bones containing no muscles or skin, and the process undoubtedly occurs after the individual's death. At this stage, the fracturing characteristics are easily recognizable because the bones behave as a rigid body (Evans, 1957). These dry bone properties of the calvaria bones determine the fracture pattern characterized by straight outlines, right angles between the cortical table and the surface of the fracture, jagged surfaces, fractures interrupted by unfused sutures and an absence of cortical delamination features (Sala et al., 2016 and references therein). The analysis of cranial fragments allowed us to

estimate that this kind of fracture is the most frequent in the SH cranial assemblage, representing 96% of the total sample (Sala et al., 2016). This indicates that postmortem fracturing is very common in the SH chamber, which is compatible with the data provided by the SH long bones (Sala, Arsuaga, Martínez, et al., 2015). Experimental studies demonstrate that fresh bone has more energy when it absorbs stress than a dry bone, which requires a much lower magnitude of force to be fractured (Evans, 1957; Gurdjian & Lissner, 1945). The most plausible scenario for the abundance of postmortem fractures in both cranial and postcranial remains is fracturing caused by overlying sediment pressure (Sala, Arsuaga, Martínez, et al., 2015; Sala et al., 2016). CT imaging has been crucial in analyzing the fracture properties in SH crania, especially for visualizing the reconstructed crania, with cranial fragments glued to each other (Figure 7).

In the case of the mandibular remains, the fractures analyzed from the 20 mandibular individuals contain properties consistent with postmortem fracturing. Condylar, angle, symphyseal, body, ascending ramus, and



FIGURE 6 Perimortem penetrating wound in Cranium-14 (upper image). Observe the detailed endocranial and ectocranial views of the injuries. Note beveling and cortical delamination around the defects along the inner table. Perimortem injuries in the frontal bone of Cranium-17 (inner image)

coronoid fractures have been documented, following the mandibular fracture nomenclature of Galloway and Wedel (2014).

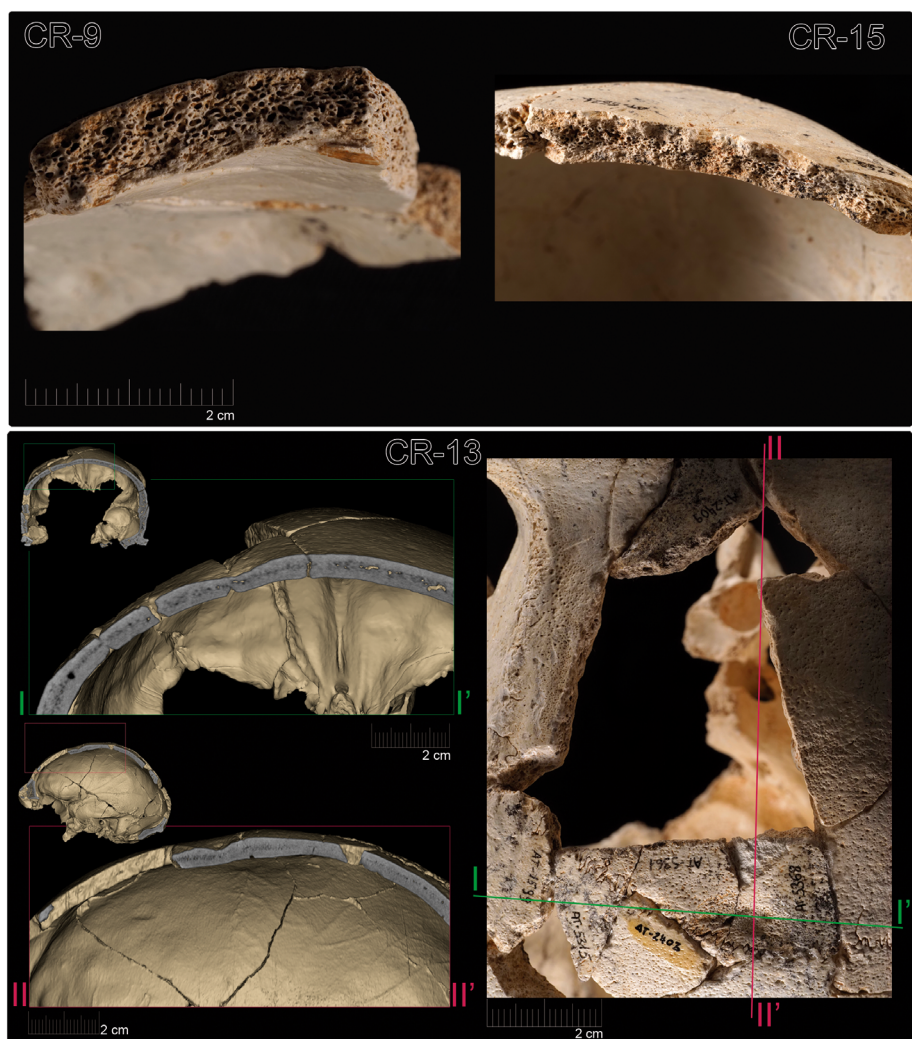
4 | BONE MODIFICATION BY BIOLOGICAL AGENTS

The SH bone assemblages, including hominin and carnivores, do not show anthropic modifications, such as cut marks, intentional fracturing in the form of percussion marks or modifications by fire. This observation rules out the anthropic intervention on human carcasses in the form of cannibalism or mortuary dismemberment. Signs of anthropic activities inside the SH chamber are absolutely absent (remains of lithic industry production or carcass processing). As well, no signs of modification by plant root etching, fungal or bacterial action, or modification by insects have been observed in the SH skulls either. Therefore, only two types of biological modifications have been identified: carnivore and rodent tooth marks.

4.1 | Carnivore activity

Regarding carnivores, despite the high incidence of tooth marks documented by Andrews and Fernández-Jalvo (1997), a low incidence (<4% of the sample) of carnivore modification has been documented by Sala, Arsuaga, et al. (2014), which is compatible with ursid scavenging of carcasses previously deposited in the SH chamber. Regarding cranial remains, four cranial fragments display marks that could be compatible with carnivore activity, though not exclusively. Scores and furrowing are not excluded in Cranium 3 (AT-444 fragment), Cranium 4 (AT-600 fragment), and Cranium 11 (AT-1159 fragment). On the other hand, a possible additional puncture was reported in Cranium 6 (fragment AT-584) (Sala, Arsuaga, et al., 2014). However, these four previously reported cases consist of isolated marks that would not indicate generalized carnivore activity in the site. In fact, the preservation of the fine bones of the splanchnocranum of several individuals is a notable exception, indicating that carnivores only negligibly

FIGURE 7 Examples of postmortem vault fractures. Note the right angles and jagged surfaces under direct observation in CR-9, CR-15, and Cr-13 and with CT images for glued cranial fragments in CR-13



affected the bone assemblage. There is, however, a distinctive case among the SH cranial sample: Cranium 5.

Cr-5 is a virtually-complete skull which preserves the neurocranium, splanchnocranum, and the complete mandible. The preservation of this specimen is exceptional, and it represents the most complete skull in the SH collection and in the hominin fossil record, indicating that no postdepositional destructive processes affected this specimen. The cranium shows several grooves crossing the sagittal suture, affecting both the left and right parietals. Similar grooves are also present on the external surface of the occipital bone (Figure 8). The width of the furrows is homogeneous along their length and is also homogeneous between contiguous furrows (see Tables S2 and S3). The furrows generally run parallel, although sometimes there are crossings and bifurcations between them (Figure 8). The cross-section of the furrows has a wide "U" morphology along their entire length. In one of the grooves, internal parallel microstriations can be distinguished and there is small triangular-shaped bone flaking at the edge of the groove (i.e., hertzian cones),

suggesting they were caused by pressure and dragging against the skull (Figure 8). However, the grooves present in the occipital do not have these hertzian cones or microstriations. They have an irregular bottom instead (Figure 8).

Different causes have been explored that could have produced these grooves: carnivore tooth marks, plant roots, insects, trauma or disease, bone abrasion by dragging against sedimentary particles or the cave wall, and scratches by bear's paws (Table S4).

1. Carnivore tooth marks. The length of the grooves is so long that it does not correspond to what is to be expected for scores made by dental cusps (Sala & Arsuaga, 2018), so this is not the most likely agent.
2. Plant roots. The typical characteristics of plant root dissolution, such as: shallow dendritic groove patterns (Behrensmeyer, 1978), smoothed-bottom of the grooves (Morlan, 1980), and sinuous trajectory (Andrews & Cook, 1985; Lyman, 1994), are not observed either, thus ruling out plant roots and acid-



FIGURE 8 Superior and posterior views of cranium 5 (Cr-5) in which the grooves affecting the right and left parietal and occipital bone can be observed. Detail and digital microscope photographs of selected areas are also shown

secreting fungi derived from plant decomposition as the cause of these grooves.

3. Insects. Diagnostic criteria for insect-induced modifications, such as star shaped pit marks, edge gnawing, and clusters of subparallel striations on the periosteal surface (Backwell et al., 2012; Kaiser, 2000), were not observed, ruling out insect activity as the origin of the linear marks on Cr-5.
4. Trauma or disease. There is no evidence of bone remodeling or signs of regeneration on the grooves;

therefore, the trauma or disease hypothesis is not supported.

5. Abrasion by dragging against sedimentary particles or the cave wall. This hypothesis, previously proposed by Andrews and Fernández-Jalvo (1997), seems improbable because the width of the pits have a U-shaped morphology, bifurcations of the grooves are observed, and the marks follow the perimeter of the crania, which would imply a rotation of the skull with respect to the cave wall.

6. Scratches by bear's paws. To evaluate this hypothesis, the features of the Cr-5 grooves have been compared with observations made in cases of bear attacks in the available literature (Baliga et al., 2012; Dhar et al., 2008; Hayashi et al., 2003; Middaugh, 1987; Nabi et al., 2009; Rasool et al., 2010). Likewise, the pattern of grooves in the skull has been compared with the paw prints preserved on the wall of the *Sala de las Oseras*, the cave chamber next to the SH (Sala et al., 2012). Bear claw marks on the cave wall usually take the form of grooves running parallel to each other, though bifurcations in the groove paths are occasionally observed (Figure S1). The distances between the grooves and their length are of the same order of magnitude as those measured in Cr-5 (Table S5). For this reason, morphologically and metrically, bear paws are the agent that best matches what was observed in Cr-5 (Baliga et al., 2012; Dhar et al., 2008; Hayashi et al., 2003; Middaugh, 1987; Nabi et al., 2009; Rasool et al., 2010).

The grooves cross both the sagittal and lambdatic suture. It should be noted that skull 5 has a pattern of obliteration of cranial sutures at stage 1, according to Meindl and Lovejoy (1985) (Pantoja-Pérez & Arsuaga, n. d.). The cranium was found at the site disarticulated by the sutures. This suggests that the grooves were produced when the skull still preserved soft tissue, that is, in the perimortem stage (no signs of regeneration are observed and therefore we discard antemortem). We, therefore, rule out the possibility that it occurred postmortem; otherwise, the marks would be interrupted by the rupture of the sutures.

4.2 | Rodents gnawing

Rodents can significantly alter bones by gnawing on them to extract calcium and phosphorus from bones (Klippel & Synstielien, 2007; Lyman, 1994). It is also

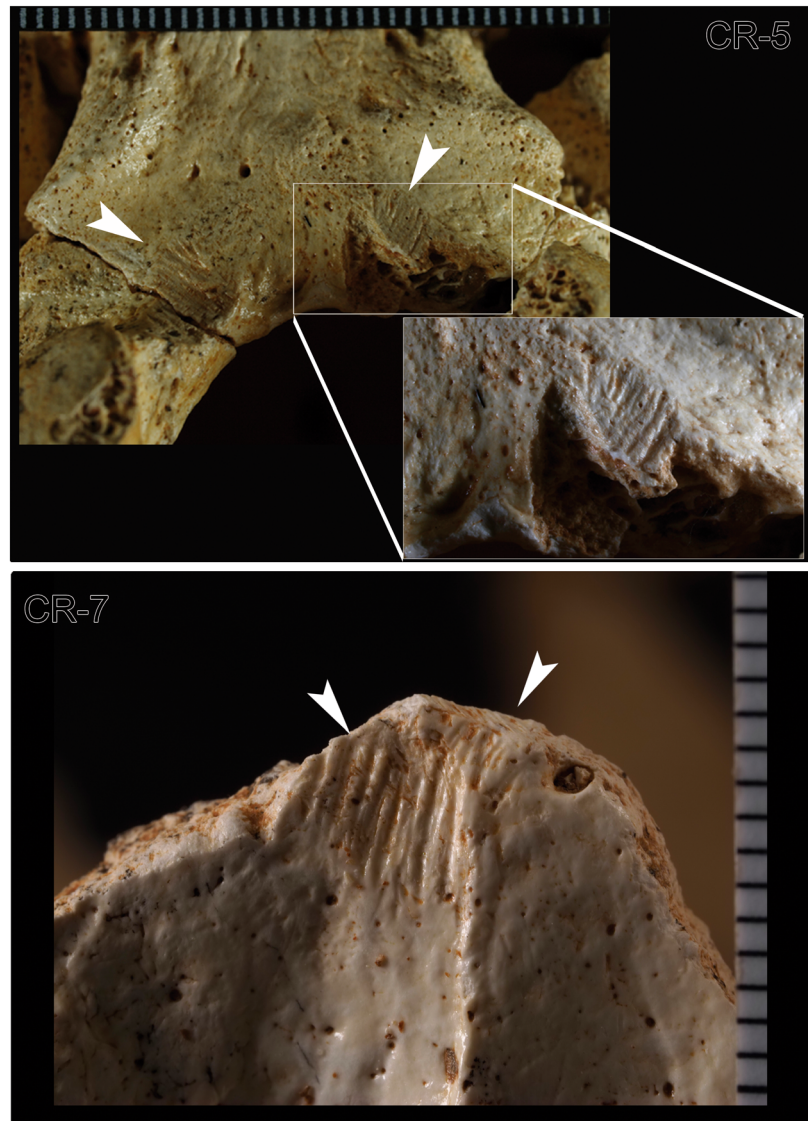


FIGURE 9 Some characteristic grooves of rodent activity in Cr-5 and Cr-7. In both cases these marks are located on the edge of the foramen magnum

possible that they may engage in this activity for the simple purpose of wearing down their continuously growing incisors by gnawing on the densest parts of the bone (Brain, 1981). During gnawing, the upper incisors are pressed into the bone to hold the head steady while the lower incisors are moved forward and upward several times, leaving readily identifiable marks (Haglund, 1997). Bone gnawing by rodents can be distinguished from other bone modification (such as carnivore tooth marks) by a straight parallel series of thin grooves that are usually paired and flat-bottomed, created by the paired incisors (Johnson, 1985; Shipman & Rose, 1983).

In the SH cranial sample, rodent damage has been identified in three cranial individuals: Cr-5, Cr-7, and Cr-9. Cr-5 and Cr-7 show a series of grooves in the foramen magnum border (Figure 9), while striae characteristic of rodent activity have been identified on the fracture edge of an occipital fragment of Cr-9. Haglund (1997) reported a spectrum of rodent damage to human remains encompassing various stages of soft tissue decomposition, including fresh, mummified soft tissues, as well as fresh and dry bones. Rodent damage in the SH cranial sample is localized in cranial regions, such as the edge of the foramen magnum, which can only be accessed after disarticulation of the first cervical vertebra (atlas), and on the edge of a postmortem cranial fracture. This would indicate the rodents' access long after the decomposition of soft tissues, disarticulation and fracturing of skeletons and, therefore, undoubtedly occurred postmortem.

5 | BONE MODIFICATION BY GEOLOGICAL AGENTS

Regarding the physical-chemical alterations that have altered the SH cranial assemblage, it should be noted that bone deformations produced by diagenetic agents have not been documented. Recrystallizations or bone mineralization have not been documented either, as manifested in the unprecedented preservation of the organic portion (mitochondrial and nuclear DNA) in the bones (Meyer et al., 2016, 2014), bearing in mind the very old chronology (c. 430–450 ka) of the fossil assemblage (Arsuaga et al., 2014; Demuro et al., 2019). No signs of subaerial exposure such as weathering have been documented. This indicates that the skeletal remains have not been exposed to the open-air atmospheric agents.

The excellent preservation of the cranial remains recovered from the *in situ* lithostratigraphic unit LU-6 (Aranburu et al., 2017) allows for the reconstruction of complete crania from fragments whose fracture edges are intact (i.e., no rounding, polishing or abrasion of bone surfaces or fracture edges; see Figure 7), indicating that



FIGURE 10 Images of cranium 1 (Cr-1) from the Sima de los Huesos showing the trampling marks and abrasion of the bone surfaces produced by cave walkers during historic times

they have not been subjected to geological processes that involve long-distance transport from outside of the SH chamber. This is consistent with the low-energy geological processes inferred from the stratigraphic and sedimentological analysis of SH (Aranburu et al., 2017). Nevertheless, a small portion (~7% of the current collection) of the hominin fossils was moved from the *in situ* lithostratigraphic unit (LU-6) to the uppermost part of the site and disturbed and trampled by nonprofessional diggers before the formal excavation period (Arsuaga et al., 1997). There are around 50 fragments from the cranial individuals recovered from this disturbed superficial unit originally known as “revuelto,” corresponding to Cr-1, Cr-2, Cr-3, Cr-7, Cr-8, Cr-12, and Cr-15. In fact, the CR-1, CR-2, and CR-8 fragments were found almost entirely in this disturbed deposit. Some of these cranial fragments have distinctive modifications of superficial exposure resulting from trampling and abrasion of the bone surfaces caused by the activity of amateur diggers looking for bear teeth in the cave during historic times. In most cases this is distinguished by the whiter coloration of the trampling and rounding of the fracture edges (Figure 10).

Excluding the aforementioned recent anthropogenic bioturbation processes, the most frequent post-depositional modifications in the SH assemblage recovered from the undisturbed *in situ* LU-6 level are, in

addition to the previously characterized postmortem fractures, those related with endokarstic environments, such as precipitation of calcite crusts and manganese oxides from cave waters.

Crusts are present in Cr-8 and CR-11. Cr-8 contains a circumferential-shaped carbonate crust (Figure 11) affecting the outer tables of the frontal and left and right parietal bones. In addition, the inner table of the left parietal is affected by a staining line arching in a parasagittal plane. These features suggest that the skull remained in a fixed position on the substrate for a long period of time, surely partially submerged in water supersaturated with CaCO_3 , where a carbonate crust of circular morphology and staining lines was formed. This cranium was later broken and its fragments were scattered throughout the surface. Almost all of the cranial fragments were recovered at the superficial disturbed level.

In addition to the transport and precipitation of carbonates in the cave environment, chemical reactions in the soil water and groundwater can mobilize other chemical elements such as iron and manganese (White &

Culver, 2012). Oxidized manganese (Mn(IV)) may be present as grain coatings in the soil or cave sediments. When biodegradation of organic matter consumes all of the available O_2 , bacteria will turn to the use of alternate electron acceptors (e.g., oxidized manganese Mn(IV)). When this element is used as an electron acceptor, it is reduced to Mn(II), which is soluble in groundwater. Dissolved Mn^{2+} may remain dissolved in cave waters or it may be reoxidized to precipitate again as Mn(IV) oxide. The presence of oxidized manganese minerals can be recognized on cave walls, speleothems or organic materials (e.g., bone porosity and/or bone surfaces) as black coatings (Marín Arroyo et al., 2008; White & Culver, 2012). In the SH, environmental conditions with a high amount of decomposing organic matter (human and bear corpses) could favor the release of the soluble form of manganese oxides. Later, this manganese could become fixed to the osseous remains due to the variation of pH on the surface of the bones, comparable to other karstic environments with skeletal remain accumulations (López-González et al., 2006; Marín Arroyo et al., 2008). In the skulls from



FIGURE 11 Detail of the circumferential-shaped carbonate crust affecting the outer table of the cranium 8 (Cr-8)

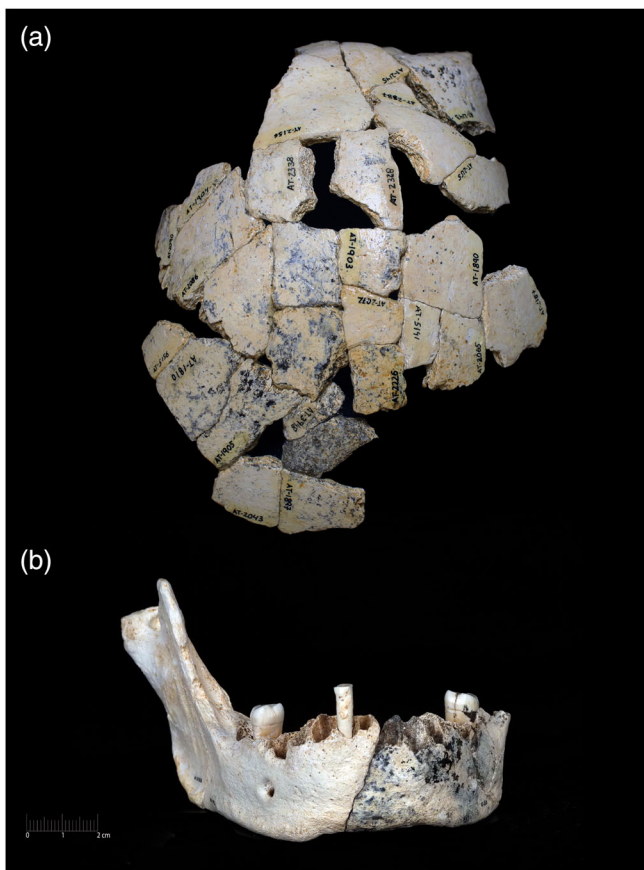


FIGURE 12 Two examples from the Sima de los Huesos collection where the different degrees of staining by manganese oxides can be observed. (a) Cr-18 frontal and parietal bone of showing that each bone fragment has different stages of impact by manganese oxides. (b) Mandible corresponding to dental individual IV in which a different pattern is observed: Its right half does not contain staining and the left half shows dark coloration due to the presence of manganese oxide precipitation

the SH, the incidence of manganese is inconsistent and affects some remains more than others. In any case, when it appears it usually manifests as small, dark brown and circular, internal stains. Sometimes the same skeletal elements have been documented with different incidences of manganese oxide staining (Figure 12), which will allow us to analyze the different postmortem taphonomic histories of these elements.

6 | CONCLUDING DISCUSSION

The collection of crania and mandibles from the SH offers an exceptional opportunity to trace taphonomic forensic aspects of a Middle Pleistocene population. The high incidence of trauma with signs of bone regeneration in the cranial bones of almost all the individuals is noteworthy. The cranial injuries are compatible with

antemortem trauma, produced by blunt impacts causing the depression of the external table of the crania. Other pathological causes that would explain these minor injuries can be ruled out. The antemortem wounds appear to affect all age categories represented in the collection and both sexes, without any evident relationship between the incidence of head injuries and age and gender categories, even considering the completeness of the individuals. Consequently, whatever agent produced this high incidence of minor lesions (intergroup violence events, accidental causes, or whatever) does not seem to affect a preferential group of the population. Therefore, it could be considered that the individuals of this Middle Pleistocene population had similar lifestyles. This type of non-fatal lesion is relatively common in the Paleolithic fossil record, including in Early Pleistocene hominins such as Gongwangling/Lantian 1 (Caspari, 1997) or Sangiran 38 (Indriati & Antón, 2010); Middle Pleistocene specimens such as Maba 1 (Wu et al., 2011), Biache 1 and 2 (Rougier, 2003) or Ceprano 1 (Mallegni et al., 2003), among others (see Wu et al., 2011 and Sala, Arsuaga, Pantoja-Pérez, et al., 2015 for inventory of specimens and references) and Late Pleistocene hominins, such as Xujiayao (Wu & Trinkaus, 2015) and numerous Neandertals and *Homo sapiens* individuals (see Wu et al., 2011 and Sala, Arsuaga, Pantoja-Pérez, et al., 2015 for inventory of specimens and references).

In addition to healed trauma, perimortem cranial alterations have been documented. First, the grooves described in Cr-5 were probably produced by bear paws in the perimortem stage; at least this is the hypothesis that best fits the data available. We cannot rule out that they were produced after death inside the site when the skull still preserved soft tissues. On the other hand, almost half of the cranial individuals have cranial fractures compatible with penetrating fractures in the perimortem phase. Six individuals have perimortem penetrating fractures in the nuchal region. The rest contain perimortem fractures in the upper portion of the left parietal bone (Cr-5 and Cr-11) or in the left half of the frontal scale (Cr-17). This pattern in the SH sample is so recurrent that it leaves little room for alternative kinds of interpretations: the presence of localized penetrating fractures and their nuchal location in these specimens is not what would be expected for accidental causes. Furthermore, the frequency of these kinds of penetrating fractures (six specimens out of nine crania with perimortem fractures) with a similar shape in the same region, suggests intentional causes rather than accidental or fortuitous occurrences. Therefore, intentionally induced injuries are the most probable hypothesis and are compatible with the other crania interpreted as cases of interpersonal violence. Recurrent acts of lethal

violence among the human groups that inhabited Atapuerca in the Middle Pleistocene thus seem evident. Although we cannot rule out that these episodes of violence also produced the antemortem injuries, the more random location of the latter prevents us from going further in interpreting their causes. However, we do not rule out that antemortem injuries could have been caused by the impact of projectiles such as rocks, resulting in a random pattern of cranial zones and affected individuals.

Cases of intergroup violence at Atapuerca have been previously documented in older chronologies. Members of *Homo antecessor* engaged in intergroup conflicts between different communities (Saladié et al., 2012; Saladié & Rodríguez-Hidalgo, 2016). However, the mortuary behavior in these two hominins seems to be quite different. Unlike *H. antecessor*, which consumed the dead individuals after the conflict (Saladié et al., 2012), the SH hominins accumulated corpses in a natural pit (Sala, Arsuaga, Pantoja-Pérez, et al., 2015).

Two modifications of biological origin have been identified in SH cranial and mandibular remains: carnivore and rodent tooth marks. In both cases the incidence is low and would have resulted from isolated events. Therefore, biological agents (carnivores or rodents) are ruled out as accumulators of the skeletons and are interpreted as postaccumulation scavengers.

The most frequent postdepositional modifications in the SH assemblage recovered from the undisturbed in situ level LU-6 are, in addition to the postmortem fractures, those related with endokarstic environments, such as precipitation of calcite crusts and manganese oxides from cave waters.

ACKNOWLEDGMENTS

In the Sima de los Huesos, an immense amount of excavation work has been conducted to recover the fossils and all the field data, to reconstruct the skulls from tiny bone fragments, to facilitate the conservation of the remains, as well as to manage all the necessary bureaucracy and administration. This research has been carried out for more than three decades by a dedicated and exceptional team. Thanks to all the members of the Sima group and to all those who have participated in this labor at some point. All the photographs of the fossils were taken by Javier Trueba from Madrid Scientific Films. We thank Maicu Ortega for her work in restoring the fossils. Ana Pantoja-Pérez received a CaixaBank - Fundación Atapuerca research fellowship. The field work at the Atapuerca sites is financed by the Junta de Castilla y León and the Atapuerca Foundation. This research is funded by Ministerio de Ciencia e Innovación PGC2018-093925-B-C33 (MCI/AEI/FEDER, UE) and is part of the DEATHREVOL project that has received

funding from the European Research Council (ERC) under the European Union's Horizon 2020 research and innovation program (Grant agreement No. 949330).

AUTHOR CONTRIBUTIONS

Noemí Sala: Conceptualization (lead); formal analysis (equal); funding acquisition (equal); methodology (equal); supervision (equal); writing – original draft (lead); writing – review & editing (lead). **Ana Pantoja-Pérez:** Formal analysis (equal); methodology (equal); writing – review and editing (equal). **Ana Gracia-Téllez:** Writing – review and editing (equal). **Juan Luis Arsuaga:** Project administration (equal); supervision (equal); writing – review and editing (equal).

ORCID

Noemí Sala  <https://orcid.org/0000-0002-0896-1493>

REFERENCES

- Andrews, P., & Cook, J. (1985). Natural modifications to bones in a temperate setting. *Man, New Series*, 20, 675–691.
- Andrews, P., & Fernández-Jalvo, Y. (1997). Surface modifications of the Sima de los Huesos fossil humans. *Journal of Human Evolution*, 33, 191–217.
- Aranburu, A., Arsuaga, J. L., & Sala, N. (2017). The stratigraphy of the Sima de los Huesos (Atapuerca, Spain) and implications for the origin of the fossil hominin accumulation. *Quaternary International*, 433, 5–21.
- Arsuaga, J. L., Carretero, J. M., Gracia, A., & Martínez, I. (1990). Taphonomical analysis of the human sample from the Sima de los Huesos middle Pleistocene site (Atapuerca/Ibeas, Spain). *Human Evolution*, 5, 505–513.
- Arsuaga, J. L., Martínez, I., Arnold, L. J., Aranburu, A., Gracia, A., Sharp, W. D., Quam, R., Falguères, C., Pantoja, A., Bischoff, J., Pozo-Rey, E., Parés, J. M., Carretero, J. M., Demuro, M., Lorenzo, C., Sala, N., Martínón-Torres, M., García, N., Alcázar de Velasco, A., ... Carbonell, E. (2014). Neandertal roots: Cranial and chronological evidence from Sima de los Huesos. *Science*, 344, 1358–1363.
- Arsuaga, J. L., Martínez, I., Gracia, A., Carretero, J. M., Lorenzo, C., García, N., & Ortega, A. I. (1997). Sima de los Huesos (Sierra de Atapuerca, Spain). The site. *Journal of Human Evolution*, 33, 109–127.
- Backwell, L. R., Parkinson, A. H., Roberts, E. M., d'Errico, F., & Huchet, J.-B. (2012). Criteria for identifying bone modification by termites in the fossil record. *Palaeogeography, Palaeoclimatology, Palaeoecology*, 337–338, 72–87.
- Baliga, S. D., Urolagin, S. B., & Balihallimath, L. J. (2012). Bear attack injury to maxillofacial region: Report of 3 cases and review of management. *Journal of Oral and Maxillofacial Surgery, Medicine, and Pathology*, 24, 198–203.
- Behrensmeyer, A. K. (1978). Taphonomic and ecologic information from bone weathering. *Paleobiology*, 4, 150–162.
- Bermúdez de Castro, J. M., Martínez, I., Gracia-Téllez, A., Martínón-Torres, M., & Arsuaga, J. L. (2021). The Sima de los Huesos middle Pleistocene hominin site (Burgos, Spain). Estimation of the number of individuals. *The Anatomical Record*, 304, 1463–1477.

- Brain, C. K. (1981). *The hunters or the hunted? An introduction to African cave taphonomy*. University of Chicago Press.
- Caspari, R. (1997). Brief communication: Evidence of pathology on the frontal bone from Gongwangling. *American Journal of Physical Anthropology*, 102, 565–568.
- de Lumley, M.-A. (2015). L'homme de Tautavel. Un *Homo erectus* européen évolué. *Homo erectus tautavelensis*. *L'Anthropologie*, 119, 303–348.
- Demuro, M., Arnold, L. J., Aranburu, A., Sala, N., & Arsuaga, J.-L. (2019). New bracketing luminescence ages constrain the Sima de los Huesos hominin fossils (Atapuerca, Spain) to MIS 12. *Journal of Human Evolution*, 131, 76–95.
- Dhar, S. A., Butt, M. F., Farooq, M., Mir, M. R., Wani, Z. A., Afzal, S., Sultan, A., & Wani, M. I. (2008). Pattern of orthopaedic injuries in bear attacks: Report from a tertiary care Centre in Kashmir. *Injury*, 39, 249–255.
- Evans, F. G. (1957). *Stress and strain in bones. Their relation to fractures and osteogenesis*. Charles C. Thomas.
- Galloway, A., & Wedel, V. L. (2014). Bones of the skull, the dentition and osseous structures of the throat. In V. L. Wedel & A. Galloway (Eds.), *Broken bones. Anthropological analysis of blunt force trauma* (2nd ed., pp. 133–160). Charles C. Thomas.
- Gómez-Olivencia, A., Quam, R., Sala, N., Bardey, M., Ohman, J. C., & Balzeau, A. (2018). La Ferrassie 1: New perspectives on a “classic” Neandertal. *Journal of Human Evolution*, 117, 13–32.
- Gracia, A., Arsuaga, J. L., Martínez, I., Martín-Francés, L., Martínón-Torres, M., Bermúdez de Castro, J. M., Bonmatí, A., & Lira, J. E. (2013). Orofacial pathology in *Homo heidelbergensis*: The case of skull 5 from the Sima de los Huesos site (Atapuerca, Spain). *Quaternary International*, 295, 83–93.
- Gurdjian, E. S., & Lissner, H. R. (1945). Deformation of the skull in head injury. A study with the stresscoat technique. *Surgery, Gynecology & Obstetrics*, 81, 679–687.
- Haglund, W. D. (1997). Rodents and human remains. In W. D. Haglund & M. H. Sorg (Eds.), *Forensic taphonomy: the postmortem fate of human remains* (pp. 405–414). CRC Press.
- Hayashi, Y., Fujisawa, H., Tohma, Y., Yamashita, J., & Inaba, H. (2003). Penetrating head injury caused by bear claws: Case report. *The Journal of trauma Injury, Infection, and Critical Care*, 55, 1178–1180.
- Indriati, E., & Antón, S. C. (2010). The calvaria of Sangiran 38, Sendangbusik, Sangiran dome, Java. *HOMO*, 61, 225–243.
- Johnson, E. (1985). Current developments in bone technology. In M. B. Schiffer (Ed.), *Advances in archaeological method and theory* (Vol. 8, pp. 157–235). Academic Press Inc.
- Kaiser, T. M. (2000). Proposed fossil insect modification to fossil mammalian bone from Plio-Pleistocene hominid-bearing deposits of Laetoli (Northern Tanzania). *Annals of the Entomological Society of America*, 93, 693–700.
- Kimmerle, E. H., & Baraybar, J. P. (2008). *Skeletal trauma: Identification of injuries resulting from human rights abuse and armed conflict*. CRC Press.
- Klippel, W. E., & Synstelien, J. A. (2007). Rodents as Taphonomic agents: Bone gnawing by Brown rats and gray squirrels. *Journal of Forensic Sciences*, 52, 765–773.
- Kremer, C., Racette, S., Dionne, C.-A., & Sauvageau, A. (2008). Discrimination of falls and blows in blunt head trauma: Systematic study of the hat brim line rule in relation to skull fractures. *Journal of Forensic Sciences*, 53, 716–719.
- Kremer, C., & Sauvageau, A. (2009). Discrimination of falls and blows in blunt head trauma: Assessment of predictability through combined criteria. *Journal of Forensic Sciences*, 54, 923–926.
- López-González, F., Grandal-d'Anglade, A., & Vidal-Romaní, J. R. (2006). Deciphering bone depositional sequences in caves through the study of manganese coatings. *Journal of Archaeological Science*, 33, 707–717.
- Lovell, N. C. (1997). Trauma analysis in paleopathology. *Yearbook of Physical Anthropology*, 40, 139–170.
- Lyman, R. L. (1994). *Vertebrate taphonomy*. Cambridge University Press.
- Mallegni, F., Carnieri, E., Bisconti, M., Tartarelli, G., Ricci, S., Biddittu, I., & Segre, A. G. (2003). *Homo cepranensis* sp. nov. and the evolution of African-European Middle Pleistocene hominids. *Comptes Rendus Palevol*, 2, 153–159.
- Mann, H. B., & Whitney, D. R. (1947). On a test of whether one of two random variables is stochastically larger than the other. *Annals of Mathematical Statistics*, 18, 50–60.
- Marín Arroyo, A. B., Landete Ruiz, M. D., Vidal Bernabeu, G., Seva Román, R., González Morales, M. R., & Straus, L. G. (2008). Archaeological implications of human-derived manganese coatings: A study of blackened bones in El Mirón cave, Cantabrian Spain. *Journal of Archaeological Science*, 35, 801–813.
- Martin, D. L., & Harrod, R. P. (2015). Bioarchaeological contributions to the study of violence. *Yearbook of Physical Anthropology*, 156, 116–145.
- Meindl, R. S., & Lovejoy, C. O. (1985). Ectocranial suture closure: A revised method for the determination of skeletal age at death based on the lateral-anterior sutures. *American Journal of Physical Anthropology*, 68, 57–66.
- Meyer, M., Arsuaga, J. L., de Filippo, C., Nagel, S., Aximu-Petri, A., Nickel, B., Martínez, I., Gracia, A., Bermúdez de Castro, J. M., Carbonell, E., Viola, B., Kelso, J., Prüfer, K., & Pääbo, S. (2016). Nuclear DNA sequences from the Middle Pleistocene Sima de los Huesos hominins. *Nature*, 531, 504–507.
- Meyer, M., Fu, Q., Aximu-Petri, A., Glocke, I., Nickel, B., Arsuaga, J.-L., Martínez, I., Gracia, A., Bermúdez de Castro, J. M., Carbonell, E., & Paabo, S. (2014). A mitochondrial genome sequence of a hominin from Sima de los Huesos. *Nature*, 505, 403–406.
- Middaugh, J. P. (1987). Human injury from bear attacks in Alaska, 1900–1985. *Alaska Medicine*, 29, 121–126.
- Moran, R. E. (1980). *Taphonomy and archaeology in the upper Pleistocene of the northern Yukon Territory: A glimpse of the peopling of the new world*. University of Ottawa Press.
- Nabi, D. G., Tak, S. R., Kangoo, K. A., & Halwai, M. A. (2009). Increasing incidence of injuries and fatalities inflicted by wild animals in Kashmir. *Injury*, 40, 87–89.
- Ortner, D. (2008). Differential diagnosis of skeletal injuries. In E. H. Kimmerle & J. P. Baraybar (Eds.), *Skeletal trauma: Identification of injuries resulting from human rights abuse and armed conflict* (pp. 21–86). CRC Press.
- Ortner, D. J. (2003). *Identification of pathological conditions in human skeletal remains*. Academic Press.
- Ortner, D. J., & Putschar, W. G. J. (1981). *Identification of pathological conditions in human skeletal remains*. Smithsonian Institution Press.
- Pantoja-Pérez A., & Arsuaga JL. (n.d.). The cranium I: Neurocranium. Anatomical record volume I. The clues of Sima de los Huesos skull remains.

- Pantoja-Pérez A, Sala N, Arsuaga JL, Pablos A, & Martínez I. (2016). Virtual assessment for the study of the cranial fractures. Application to the Sima de los Huesos hominin crania. Sixth Annual Meeting of the European Society for the Study of Human Evolution (ESHE). European Society for the Study of Human Evolution.
- Pérez, P. J. (1989). Paleopatología del hombre fósil de Ibeas (Sierra de Atapuerca, Burgos). In E. Rebato & R. Calderón (Eds.), *Actas del VI Congreso Español de Antropología Biológica* (Bilbao, 1989) (pp. 403–411). Universidad del País Vasco.
- Pérez, P. J. (1991). Evidence of disease and trauma in the fossil man from Atapuerca-Ibeas (Burgos, Spain). *International Journal of Osteoarchaeology*, 1, 253–257.
- Pérez, P. J., Gracia, A., Martínez, I., & Arsuaga, J. L. (1997). Paleopathological evidence of the cranial remains from the Sima de los Huesos Middle Pleistocene site (Sierra de Atapuerca, Spain). Description and preliminary inferences. *Journal of Human Evolution*, 33, 409–421.
- QGIS.org. (2021). *QGIS 3.16. Geographic information system user guide*. QGIS Association.
- Rasool, A., Wani, A. H., Darzi, M. A., Zaroo, M. I., Iqbal, S., Bashir, S. A., Rashid, S., & Lone, R. A. (2010). Incidence and pattern of bear maul injuries in Kashmir. *Injury*, 41, 116–119.
- Rougier, H. (2003). Étude descriptive et comparative de Biache-Saint-Vaast 1 (Biache-Saint-Vaast, Pas-de-Calais, France). In *Sciences du Vivant, Géosciences et Sciences de l'Environnement* (Vol. 1, p. 418). L'Université Bordeaux.
- Sala, N., & Arsuaga, J. L. (2018). Regarding beasts and humans: a review of taphonomic works with living carnivores. *Quaternary International*, 466, 131–140.
- Sala N, Arsuaga JL, Martínez I, Gracia-Téllez A. (2012). Taphonomical analysis of the cranium 5 from the Sima de los Huesos site (Atapuerca, Spain). Second Annual Meeting of the European Society for the Study of Human Evolution.
- Sala, N., Arsuaga, J. L., Martínez, I., & Gracia-Téllez, A. (2014). Carnivore activity in the Sima de los Huesos (Atapuerca, Spain) hominin sample. *Quaternary Science Reviews*, 97, 71–83.
- Sala, N., Arsuaga, J. L., Martínez, I., & Gracia-Téllez, A. (2015). Breakage patterns in Sima de los Huesos (Atapuerca, Spain) hominin sample. *Journal of Archaeological Science*, 55, 113–121.
- Sala, N., Arsuaga, J. L., Pantoja-Pérez, A., Pablos, A., Martínez, I., Quam, R. M., Gómez-Olivencia, A., Bermúdez de Castro, J. M., & Carbonell, E. (2015). Lethal interpersonal violence in the middle Pleistocene. *PLoS One*, 10, e0126589.
- Sala, N., Pantoja, A., Martínez, I., Gracia-Téllez, A., & Arsuaga, J. L. (2014). The Sima de los Huesos crania. Taphonomic analysis. In D. Bassi & R. Posenato (Eds.), *7th International Meeting on Taphonomy and Fossilization Ferrara 2014*. Annali dell'Università di Ferrara, Sez. Fisica e Scienze della Terra.
- Sala, N., Pantoja-Pérez, A., Arsuaga, J. L., Pablos, A., & Martínez, I. (2016). The Sima de los Huesos crania: Analysis of the cranial breakage patterns. *Journal of Archaeological Science*, 72, 25–43.
- Saladié, P., Huguet, R., Rodríguez-Hidalgo, A., Cáceres, I., Esteban-Nadal, M., Arsuaga, J. L., Bermúdez de Castro, J. M., & Carbonell, E. (2012). Intergroup cannibalism in the European early Pleistocene: The range expansion and imbalance of power hypotheses. *Journal of Human Evolution*, 63, 682–695.
- Saladié, P., & Rodríguez-Hidalgo, A. (2016). Archaeological evidence for cannibalism in prehistoric Western Europe: From *Homo antecessor* to the bronze age. *Journal of Archaeological Method and Theory*, 24, 1034–1071.
- Sanz, M., Sala, N., Daura, J., Pantoja-Pérez, A., Santos, E., Zilhão, J., & Arsuaga, J. L. (2018). Taphonomic inferences about middle Pleistocene hominins: The human cranium of Gruta da Aroeira (Portugal). *American Journal of Physical Anthropology*, 167, 615–627.
- Shang, H., & Trinkaus, E. (2008). An ectocranial lesion on the middle Pleistocene human cranium from Hulu cave, Nanjing, China. *American Journal of Physical Anthropology*, 135, 431–437.
- Shipman, P., & Rose, J. (1983). Early hominid hunting, butchering, and carcass-processing behaviors: Approaches to the fossil record. *Journal of Anthropological Archaeology*, 2, 57–98.
- Thomas, L. M. (1984). Injury of the head and cervical spine. In R. H. Mathog (Ed.), *Maxillofacial trauma* (pp. 74–78). Williams & Wilkins.
- Ubelaker, D. H., & Adams, B. J. (1995). Differentiation of perimortem and postmortem trauma using taphonomic indicators. *Journal of Forensic Sciences*, 40, 509–512.
- White, W. B., & Culver, D. C. (2012). *Encyclopedia of caves*. Academic Press.
- Wu, J. H., & Trinkaus, E. (2015). Neurocranial trauma in the late archaic human remains from Xujiayao, northern China. *International Journal of Osteoarchaeology*, 25, 245–252.
- Wu, X.-J., Schepartz, L. A., Liu, W., & Trinkaus, E. (2011). Antemortem trauma and survival in the late middle Pleistocene human cranium from Maba, South China. *Proceedings of the National Academy of Sciences of the United States of America*, 108, 19558–19562.

SUPPORTING INFORMATION

Additional supporting information may be found in the online version of the article at the publisher's website.

How to cite this article: Sala, N., Pantoja-Pérez, A., Gracia, A., & Arsuaga, J. L. (2022). Taphonomic-forensic analysis of the hominin skulls from the Sima de los Huesos. *The Anatomical Record*, 1–19. <https://doi.org/10.1002/ar.24883>